High-throughput screening of metal – Organic frameworks for CO_2 and CH_4 separation in the presence of water

Justyna Rogacka[a], Agnieszka Seremak[a], Azahara Luna-Triguero[b], Filip Formalik[a], Ismael Matito-Martos[b], Lucyna Firlej[a,c,*], Sofia Calero[b,d], Bogdan Kuchta[a,e]

[a] *Department of Micro, Nano and Bioprocess Engineering, Faculty of Chemistry Wroclaw University of Science and Technology, Wroclaw, Poland*
[b] *Department of Physical, Chemical, and Natural Systems, University Pablo de Olavide, Seville, Spain*
[c] *Charles Coulomb Laboratory, University of Montpellier, CNRS, Montpellier, France*
[d] *Materials Simulation and Modelling, Department of Applied Physics, Eindhoven University of Technology5600MB Eindhoven, the Netherlands*
[e] *MADIREL, Aix-Marseille University, CNRS, Marseille, France*

Competitive adsorption of water is an important issue in the adsorption-based industrial processes of bio- and flue gases separation. The dehumidification of gases prior to separation would increase process complexity and lower its economic interest. In this work, large-scale computational screening was applied to identify Metal-Organic Frameworks (MOFs) structures which exhibit high CO_2/CH_4 selectivity and total loading higher than 0.5 mol/kg (in the presence of water). High-throughput Grand Canonical Monte Carlo (GCMC) screening of nearly 3000 existing MOF materials was carried out. Initial selection assumed fixed values of pore limiting diameter (PLD) and Henry's constant for water and allowed one to preselect 764 structures. After GCMC simulations carried for 50/50 CO_2/CH_4 mixture, at ambient conditions (p = 1 bar, T = 298 K), and variable gas humidity (0%, 5%, 30% and 40%) the final selection revealed 13 most promising MOFs structures. We focused on analysis of the correlations between the properties of the selected MOFs and the separation selectivity. We show that the selectivity is a complex function of the porous materials characteristics and finding selective sorbent, performing well in dry and wet conditions requires careful analysis of available MOFs.

* Corresponding author at: Charles Coulomb Laboratory (L2C), University of Montpellier, Pl. E.Bataillon, cc. 026, 34095 Montpellier, France.
E-mail address: lucyna.firlej@umontpellier.fr (L. Firlej).

1. Introduction

According to International Energy Agency (IEA Statistics) [1], today 80 percent of the world's energy comes from fossil fuels. As a result of fossil fuel burning the atmospheric concentration of CO_2, one of the major greenhouse gases, has dangerously increased [2]. To reduce the rapid changes of Earth atmosphere composition different CO_2 capture and storage (CCS) strategies have been proposed [2–9]. They address all stages of fossil fuel exploitation, form pre-combustion treatment, through combustion optimization and post-combustion CO_2 capture [2]. The post-combustion CO_2 separation from other combustion gases (by filtration or absorption) for its subsequent sequestration and/or utilization has received a lot of interest [10–15]. The energy-efficient, adsorption-based solutions are particularly promising [10,12,14,16–20]. However, the generalized use of adsorption based technologies requires the development of selective, high-performance CO_2 sorbents, withstanding variable working conditions [21]. For the best outcome, they should enable guest molecules to diffuse rapidly into the pore network and possess moderate heat of CO_2 adsorption to ensure efficient gas separation and sorbent regeneration.

Various porous sorbents were proposed and analyzed in the past: activated carbon [22–24], carbon molecular sieves (CMS) [25–27], polymers [28–30], aluminophosphates (AlPOs) [31–33] and aluminosilicates (zeolites) [24,34], covalent-organic frameworks (COFs) [35]. Recently [34], a new class of porous materials, metal–organic frameworks (MOFs), has proved its potential to be used in the gas separation or storage [17,36–46]. Due to their unique physical properties (tuneability of their crystalline structure, high porosity and ultra-high surface area), MOFs are considered as a promising class of sorbents for separation and storage of various gases, including carbon dioxide and methane [41,47–50].

Numerical screenings of MOFs for selective adsorption of greenhouse gases were performed in the past for various gases combinations: CO_2/H_2O and $CO_2/H_2O/N_2$ [51], CH_4/N_2, CH_4/CO_2, CH_4/H_2S, and CH_4/NH_3 [49]. Huang et al. [52] investigated the capture of CO_2 from CH_4/CO_2 mixture in 25 well-known MOFs and showed that the preferential CO_2 adsorption in a framework in humid conditions depends on the relative strength of water and CO_2 attraction by the framework. When the interaction between H_2O and MOF framework is strong, water saturates the highly attractive adsorption sites, and the CO_2 uptake is low. Similarly, Yu et al. [53] showed that CO_2 adsorption in Mg-MOF-74 decreases with increased humidity; the density functional theory (DFT) calculations showed that the reduction of CO_2 adsorption energy was caused by H_2O binding to the unsaturated metal sites. Han et al. [54] studied stability and CO_2/N_2 sorption selectivity of seven MOFs, and showed that some of studied structures remain stable and selective in humid conditions. Adsorption of small molecules (CO_2, H_2O, H_2 and CH_4) in 25 different metal-substituted MOF-74 was studied by Canepa et al. [55]. Using DFT calculations the authors demonstrated the impact of humidity on the separation capacity of MOF structures. Many works were devoted to identifying highly selective materials for CO_2 sorption in the presence of water. Li et al. [51] calculated the ratio of Henry s constants k_H for CO_2 and H_2O adsorption for large number of MOF structures and selected 13 the most promising frameworks (for which $k_H(CO_2)/k_H$ (H_2O) ratio was the largest). For these structures Grand Canonical Monte Carlo (GCMC) simulations of binary CO_2/H_2O and ternary $CO_2/H_2O/N_2$ mixtures adsorption were then carried out, in highly humid environment (80% relative humidity). The authors stressed that the partial charges distribution on MOF should be determined very precisely to reach high quality, quantitative results in simulations explicitly containing water molecules. The problem of partial charges was also noted by Altintas et al. [56] in the context of simulations of CO_2 adsorption in MOFs. The authors concluded that to avoid time consuming DFT calculations of partial charges (DDEC, density-derived electrostatic and chemical method), extended Qeq (charge equilibration method) can be used. However, both methodologies produce different charge distributions that in turn lead to different uptakes, working capacities and selectivity, especially in MOFs with narrow pores. These differences can be neglected as long as rapid screening of large number of structures is prospected; to narrow down the analysis of sorption properties of down-selected structures more accurate charges assignment is necessary.

An extensive review on water adsorption in MOFs, and stability of MOFs after exposure to moisture was written by Canivet et al. [57]. The authors concluded that to ensure the stability of MOF structure in humid environment the ligands should tightly shield the MOFs' metallic centers, and the interaction metal–ligand should be strong. This can be achieved when very basic ligands are used together with very acidic metals (as, for example, in Cr-MIL-101, where Cr^{3+} is used together with azolates). Keskin group performed screening of 13 MOFs for $CO_2/H_2O/CH_4$ and $CO_2/H_2O/N_2$ separations which showed that addition of water to the binary mixtures significantly affects the separation performance [58]. The same group synthesized 2 MOFs (Al-PMOF and Al-PyrMOF) to check for CO_2/N_2 selectivity in wet flue gas, after first finding the most promising structures with parallel aromatic rings via reverse-screening of 8,325 MOF database [59]. Furthermore, Keskin et al. published a series of papers on screening of a database containing 3857 MOF structures for capacity to separate CO_2/H_2 [60], H_2/N_2 [61] and CO_2/N_2 [62] and CO_2/CH_4 [63] gas mixtures. The most promising structures in each category were used as fillers in mixed matrix membranes and the separation they provided was further investigated.

The largest screening of MOF structures was carried out by Ahmed et al. who analyzed 493 459 frameworks to find the best material for hydrogen storage [64]. The most promising structures: SNU-70, UMCM-9 and NU-100 were further analyzed at 77 K and the pressure range 5–100 bar using GCMC methodology.

Experimental screenings of MOFs were also performed, although on a much smaller scale. Evans et al. [65] performed binary gas breakthrough measurements of dynamic capacity of CO and N_2 adsorption in 10 MOFs, to verify their performance in CO/N_2 separation, and applicability in petrochemical industry. Han et al. [66] investigated CO_2 and N_2 adsorption and diffusion in 8 selected MOFs, in dry and humid conditions. The most promising material showed selectivity ratio (the ratio of the adsorbed amount of CO_2 with respect to N_2) equal 152. Chanut et al. [67] screened 45 MOFs for water impact on CO_2 adsorption, and identified four highly selective structures: UiO-66-NH_2, UiO-66-2Me, MIL-127(Fe) ad MIL-96(Al). These MOFs showed fairly constant CO_2 uptake with increasing relative gas humidity (2–14% R_H). Authors also show that the CO_2 uptake decreases in wet samples proportionally to the structure's value of Henry constant k_H for water. This result indicated that strong framework affinity to water is not favorable for high CO_2 adsorption in the structure.

To the best of our knowledge the large-scale analysis of MOFs capacity to efficiently separate carbon dioxide and methane mixtures in the presence of water was never performed. Therefore, to identify potentially high-performing MOFs for biogas or flue gas purification in humid conditions we scrutinized > 2,900 structures from the CoRE-MOF database (version 2016) [68]. This library contains experimentally determined MOF structures that are computation-ready. For 2932 structures that possesses pores large enough to adsorb CO_2 the numerical analysis of selective adsorption of CO_2 from equimolar CO_2/CH_4 mixture in dry and wet conditions has been carried out. The choice of best (most selective) MOF structures was based on the results of a two-steps procedure involving GCMC simulations of adsorption isotherms with RASPA code. This approach has allowed us to designate 13 structures that perform the best in variable humidity conditions. 3 of them show at the same time high CO_2 uptake during adsorption from CO_2/CH_4 mixture.

2. Methodology

The adopted methodology is summarized in the Fig. 1. The

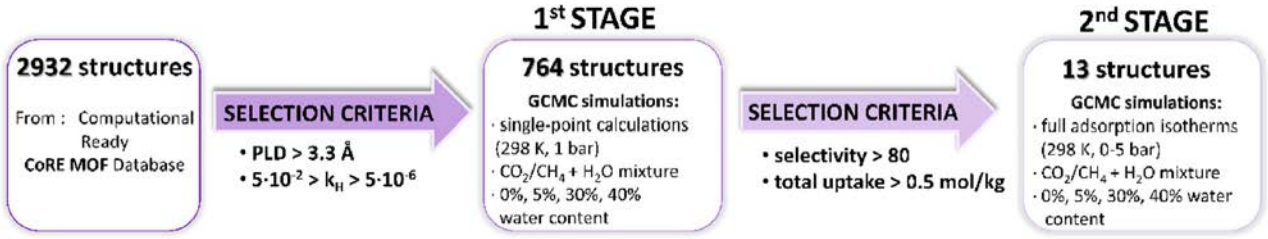

Fig. 1. Schematic representation of numerical screening protocol.

Computational Ready (CoRE MOF 2014-DDEC) database [68] was used as a reservoir of MOFs structures for the selection of materials with high CO_2/CH_4 selectivity ratio. We considered only solvent-free structures provided with charges calculated using DDEC method, ready to implement in simulations of adsorption. The 2932 experimental MOFs structures that fulfilled this condition were chosen for further analysis.

The initial selection was made with respect to the values of 2 parameters: the pore limiting diameter (PLD), and Henry constant (k_H) for water adsorption. PLD is defined as the maximum size of a sphere that can move through the structure without hindrance. As the kinetic diameter of carbon dioxide is $\sigma = 3.3$ Å, therefore only structures with PLD > 3.3 Å were chosen for further study. This geometric selection is essential, as optimal permeation and diffusion of gases through the material must be ensured in any technological process. Water affinity of the frameworks was chosen to be in the medium range, to eliminate structures that are too hydrophilic or too hydrophobic. The notion of the 'medium range' has been defined by Matito-Martos et al. [69] as contained between the limiting values ($5{\cdot}10^{-6}$, $5{\cdot}10^{-2}$) mol/kg·Pa. The hydrophobic materials show the $k_H < 5{\cdot}10^{-6}$ mol/kg·Pa, whereas for hydrophilic materials $k_H > 5{\cdot}10^{-2}$ mol/kg·Pa. Medium affinity towards water guarantees that adsorption sites would not be occupied exclusively by water at ambient conditions; at the same time water is not totally excluded from the pore volume. These two criteria allowed a limitation of the initially selected MOFs to 764 structures (after an additional removing of structures referenced twice, especially when they were imported from Cambridge Crystal Structure Database CCDS [70], or containing erroneous data). The list of detected inconsistencies is given in Supporting Information (SI).

The numerical screening protocol was based on the calculations of adsorption isotherms using Grand Canonical Monte Carlo methodology implemented in the state-of-the-art RASPA code [71]. The inter- and intra- molecular interactions were calculated using 6–12 Lennard-Jones (LJ) potentials, truncated at a *cutoff* distance of 12 Å. The LJ parameters for MOFs were taken from DREIDING [72] (for organic linkers) and UFF [71] (for metal sites) forcefields. For CO_2 the all atoms model has been used, whereas CH_4 was represented as single united atom model. The LJ parameters for both gases were taken from Ref. [73]. The all atom TIP4p model [74] was used for water. MOFs' structures were considered as rigid in the simulations. Lorentz-Berthelot mixing rules were applied to parametrize adsorbate-adsorbent interactions. Coulomb potential and Ewald summation were used to account for electrostatic interactions in the systems. Each GCMC simulation contained 10 000 equilibration and 200 000 production cycles (number of MC steps per cycle is equal to the total number of molecules in the system, however, not < 20). The number of chosen production cycles guarantees that the calculated mean values converge to an equilibrium loading for multicomponent adsorption simulations. In each cycle translation, rotation, regrow, identity change and swap moves were performed.

The 1st stage of screening consisted in calculations of the adsorbed amount at single (p, T) point (p = 1 bar, T = 298 K), to limit computational time. First, adsorption of an equimolar mixture of CO_2 and CH_4 (50:50) was calculated to obtain total loading (defined as a sum of adsorbed amount of each gas, $T_{loading} = n_{CO_2} + n_{CH_4}$, in mol/kg), and adsorption selectivity of each material of CO_2 over CH_4 ($S_A = n_{CO_2}/n_{CH_4}$). Then, water molecules have been added to the initial gas mixture to reach 5%, 30% and 40% of humidity of the adsorbent. Humidity in this work is defined as a fraction of the available pore volume occupied by water molecules. This quantity was estimated for each MOF structure in the following way: first, prior to simulations, the number of water molecules that can fit the available pore volume (as defined by helium void fraction) has been calculated, and the number of water molecules necessary to achieve the desired humidity level was determined. This amount of water molecules was then inserted into the structure during simulations. Such procedure allowed for rapid evaluation of the potential evolution of selectivity of each framework with increasing water content. More details about the process followed for the addition of specific amount of solvent within the pores can be found in literature [35]. In consequence, for the next step of screening we have chosen 13 structures showing the total CO_2/CH_4 loading above 0.5 mol/kg, and the high selectivity ratio (above 80) at least at one of the studied hydration degrees.

In the 2nd stage of screening, for the thirteen preselected MOFs structures, the simulations of full adsorption isotherms were performed, at ambient temperature (T = 298 K) and in the pressure range from 0 to 5 bar. Four series of simulations were carried out: for 0%, 5%, 30% and 40% of humidity. For all selected structures, the simulations of water adsorption were also performed, to serve as reference for selectivity analysis. From the simulations at low pressures the values of isosteric heats of adsorption for CO_2 and CH_4 at 298 K were determined.

3. Results and discussion

3.1. 1st stage of screening.

Fig. 2 shows the variation of the total adsorption of the CO_2/CH_4 mixture in the function of PLD size of 764 preselected MOFs structures, for different water content. The comparison of four graphs shows that the adsorption capacity decreases as the content of moisture in the material increases. The highest total adsorption of the dry gas mixture is 8.93 mol/kg and decreases to only 3.73 mol/kg when the structure contains 40% of humidity. It proves that in the last case the major part of the available pore space is taken by inserted water molecules. Moreover, for all water contents the highest total loadings were observed not in the structures with biggest pores (PLD > 9), but in those with the smaller ones (PLD < 9). This high total loading results from stronger interactions with (closer) adsorption sites, and from additivity of their values. We concluded that the sorbents with smaller pore diameters are more suitable for CO_2/CH_4 adsorption at ambient temperature and pressure; in consequence the large PLD structures (PLD > 9) were removed from the further study.

Fig. 3 shows the total adsorbed amount/selectivity diagrams at different humidity contents. The graphs illustrate the adopted criteria of structures' selection for the 2nd stage of screening. Only those structure that simultaneously show very good selectivity (above 80), and high total loading of $CH_4 + CO_2$ (> 0.5 mol/kg) have been selected. This ensures that a non-negligible amount of both gases would be adsorbed, and selectivity calculations would not be susceptible to errors resulting from division of two very small numbers (as it is the

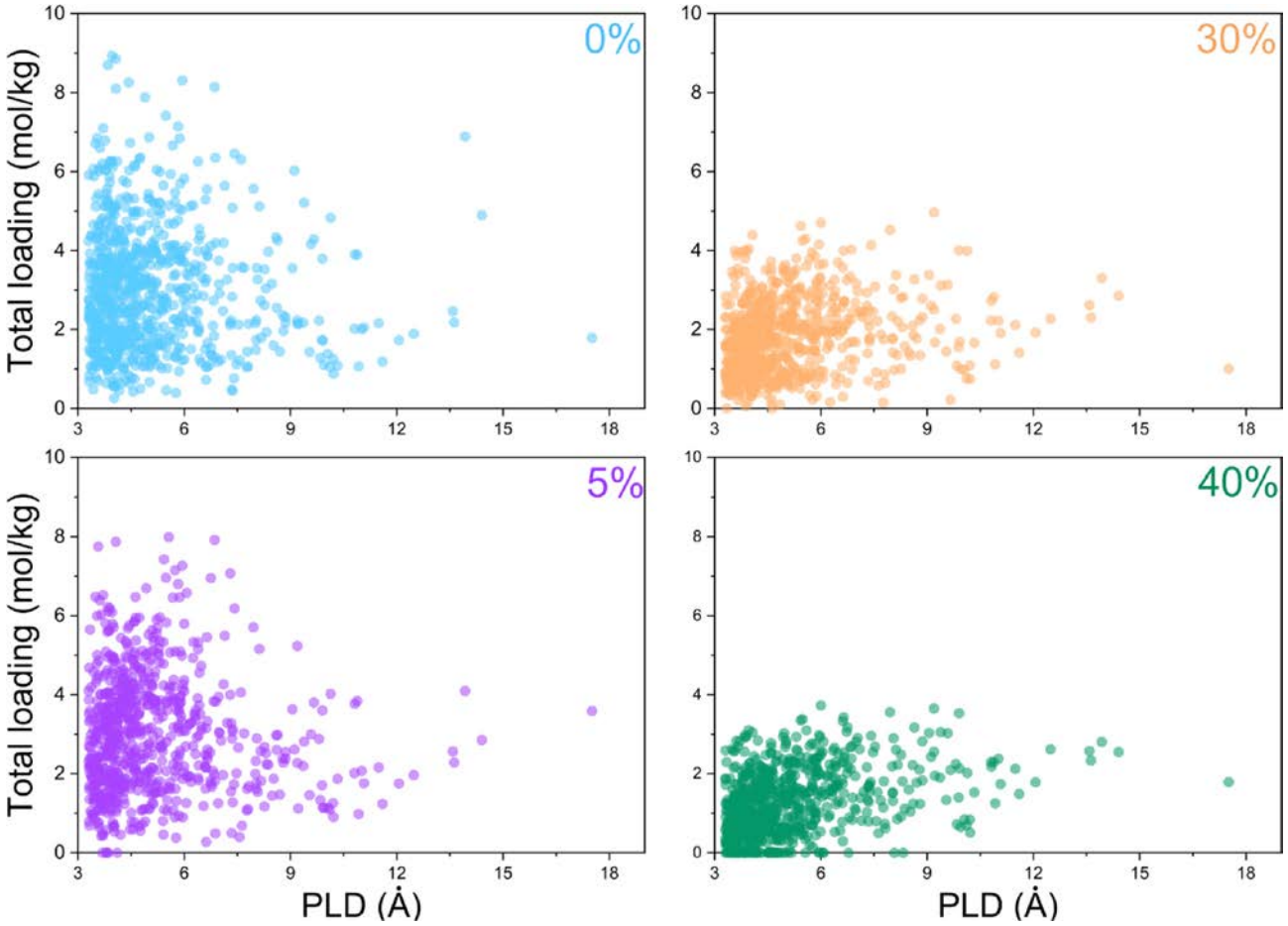

Fig. 2. The variation of the total adsorption of the CO_2/CH_4 mixture in the function of PLD size of 764 preselected MOFs structures, for different water contents (0%, 5%, 30%, 40%).

case for NARTIL structure which has selectivity of 797 at 40% of humidity, (see Fig. 3) resulting from almost negligible total loading). Altogether, 13 MOF structures were selected for 2nd stage of screening, even if they performed well in only one specific humidity condition. Half of them (GUJPEG01, LOFZUB, KIDDOS, KINKAV, CEHVIX, UDICAN) remain highly selective even if the humidity concentration in the samples is high (30% and 40%).

It is important to stress out that not all of the materials that show very good potential for separation were actually synthesized. CEHWIX [75] was generated theoretically using machine learning protocol, and UDICAN [76] is an intermediate structure in the crystallization process of some of structures not selected by this screening. Although these materials cannot be the sorbent candidates for real applications, the present analysis reveals their potential and unique properties. We continue analyzing them in the 2nd stage of screening.

3.2. 2nd stage of screening.

Table 1 gathers basic information about the 13 MOF structures selected for the 2nd stage of screening for best sorbents for CO_2/CH_4 separation in presence of water. MOF structures are listed in order of decreasing Henry's constant k_H for water adsorption. The dispersion of k_H is large, roughly 3 orders of magnitude. All materials also show a large dispersion of the unit cell volumes. 5 out of 13 structures contain Zn atom in the metallic center, but the structures with other metals (Er, Ga, Cd, Bi) are present as well. Nitrogen atom is present in the linkers of 9 out of 13 structures. We relate this observation to the previous study [19] showing that imprinting alkaline nitrogen groups on polyethyleneimine improves separation quality and absorption capacity of industrial CO_2 storage tanks. The alkaline nitrogen group presence can probably partially explain the high affinity of these selected MOF structures towards CO_2.

We noticed that LOFZUB structure deposited in the CoRE-MOF database is actually not a MOF but an AlPO-type zeolite; however, as it shows very high total loading and high selectivity (> 100) we decided to include here the analysis of this material as well. GOMRAC structure (Fig. 3) is an AlPO as well, but it was not included in further investigations due to poorer performance than LOFZUB structure.

For all selected structures, the affinity for water, characterized by k_H constant, does not impact the separation process. Theoretical water capacity of each structure, calculated from geometrically available space for adsorption, and simulated water uptake at $T = 298$ K and maximal pressure of 5 bar are given in Table 1. The comparison of these values shows that in most of the selected structures water fills $< 40\%$ of the available space, even at pressure of 5 bar. As the pressures usually applied in separation systems are much lower, the risk of overfilling MOF structures with water during actual process is very low.

Fig. 4 presents the possible adsorption surfaces (in violet) in all selected structures. They were generated using iRASPA software [88] from the results of short-time simulations of single CH_4 molecule adsorption in the structures. Changing probing molecule to CO_2 did not change significantly neither the shape nor the size of adsorption surface. This allowed for a visualization of both preferential adsorption sites and the pathway for CO_2/CH_4 diffusion through the pores structure.

Fig. 5 shows pore size distribution for the selected structures. Most of them have the pore diameter > 3.8 Å, the kinetic diameter of methane. It proves that the selectivity is not defined by the geometric

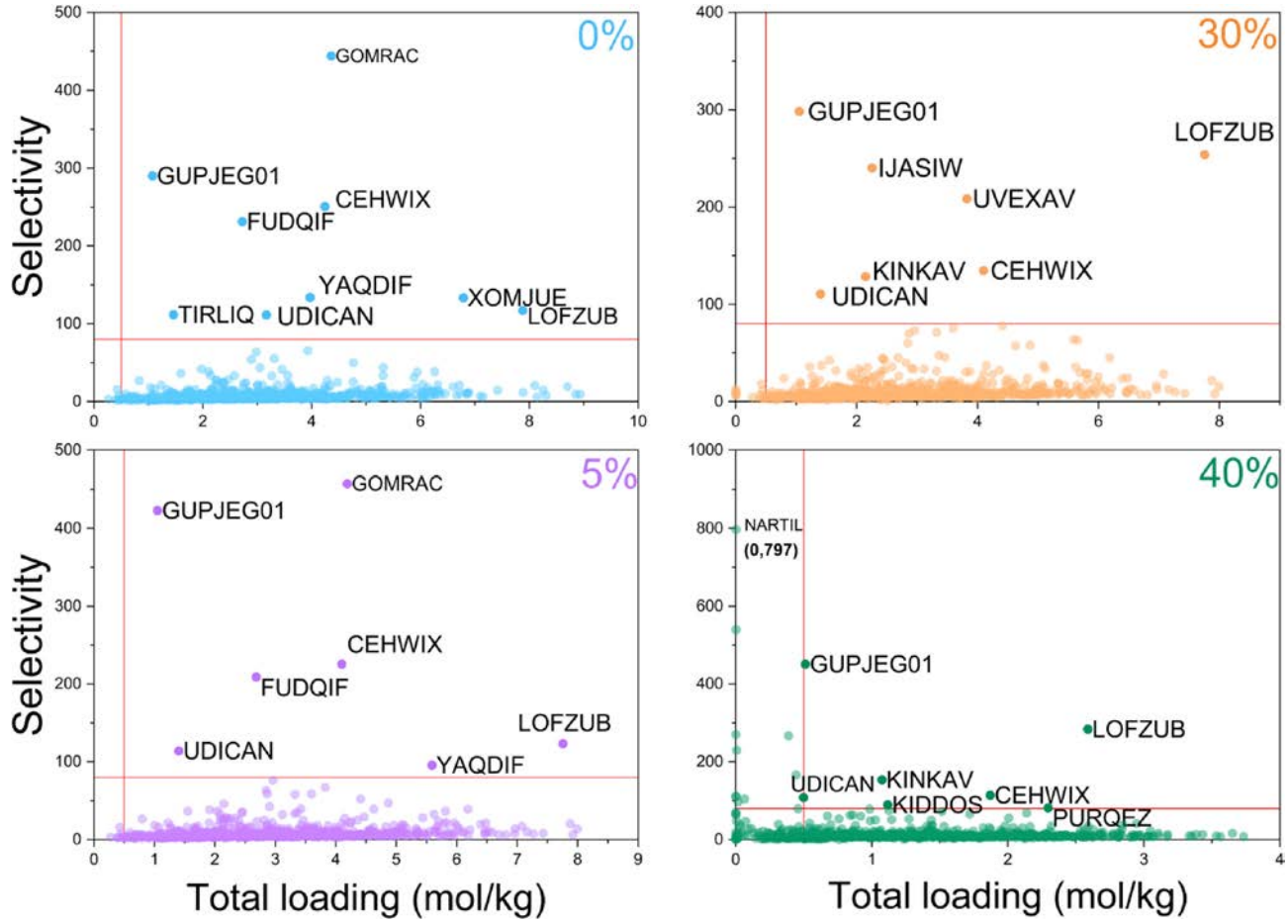

Fig. 3. The variation of the selectivity of the CO_2/CH_4 mixture in the function of total adsorption of CO_2 + CH_4 for 764 preselected MOFs structures, for different water contents (0%, 5%, 30%, 40%). Red lines indicate the reference levels for selection of structures for the second stage of screening. (For interpretation of the references to colour in this figure legend, the reader is referred to the web version of this article.)

parameters of the structure only. LOFZUB structure that contains the largest pores is highly selective at all humidity conditions.

Fig. 6a shows the heats of adsorption of CO_2 and CH_4 calculated from energy fluctuations in simulations of the single gas adsorption at very low pressure, for each selected structure [89]. The analysis of the diagrams brings to the light two important facts. First, both methane and carbon dioxide are strongly adsorbed by all structures (their adsorption heats are > 15 kJ/mol). The heats of CO_2 adsorption values are in the same range as for other largely studied MOFs like HKUST-1 (30 kJ/mol), MIL-100 (62 kJ/mol), and for other porous structures like zeolite 13X (34 kJ/mol), and MEA solution (84 kJ/mol) [90]. Second, the difference in heats of adsorption between

Table 1
Reference codes, chemical formulas and unit cell volume of MOFs selected for the 2nd stage of screening, presented in order of increasing values of Henry constant k_H for water. Theoretical (geometrical water capacity in (mol per unit cell, mol/uc) is compared to the calculated (GCMC) water amount adsorbed at 5 bar and 298 K. The humidity at 5 bar is calculated as the ratio between calculated water amount at (5 bar, 298 K) and theoretical water capacity of the structure. Bolded numbers indicate structures with humidity > 40% in these conditions.

Ref. code	Chemical formula	Unit cell volume Å^3	k_H mol/kg·Pa	Theoretical water capacity mol/uc	Calculated water amount adsorbed at 5 bar mol/uc	Humidity at 5 bar %	Ref
KINKAV	$C_{40}H_{36}N_6O_7$**Zn**	1987	$4.51 \cdot 10^{-2}$	35	11.0	31.5	[77]
CEHWIX	**Ni**$H_3C_5N_2ClO_2$	929	$4.44 \cdot 10^{-2}$	33	9.5	28.9	[75]
KIDDOS	$C_{66}H_{92}N_{14}O_{37}S_6$**Zn**$_6$	4316	$2.34 \cdot 10^{-2}$	149	52.5	35.2	[78]
YADQIF	**Cd**$H_{16}(C_4O)_8$	3744	$2.18 \cdot 10^{-2}$	70	49.2	70.3	[79]
UVEXAV	**Ga**$_2H_5C_5O_8$	553	$2.09 \cdot 10^{-2}$	55	5.8	10.5	[80]
FUDQIF	**Zn**$SiH_8C_8(N_2F_3)_2$	388	$8.64 \cdot 10^{-3}$	31	3.3	10.6	[81]
UDICAN	**Bi**$_6H_6C_{18}O_{17}$	3229	$3.62 \cdot 10^{-3}$	70	28.5	40.7	[76]
LOFZUB	**AlPO$_4$**	3332	$3.55 \cdot 10^{-3}$	142	59.0	41.5	[82]
TIRLIQ	**Zn**$_3H_{22}C_{34}(NO_6)_2$	4181	$1.45 \cdot 10^{-3}$	54	35.7	66.2	[83]
XOMJUE	**Er**$H_{32}C_{44}N(ClO_3)_3$	5417	$8.21 \cdot 10^{-4}$	95	51.0	53.7	[84]
PURQEZ	**Zn**$H_6(CO)_8$	1564	$1.19 \cdot 10^{-4}$	58	20.5	35.3	[85]
IJASIW	**Er**$H_{14}C_{24}(NO_3)_2$	1239	$6.43 \cdot 10^{-5}$	41	8.5	20.7	[86]
GUPJEG01	**Mn**$H_6C_{12}(NO_2)_2$	636	$4.88 \cdot 10^{-5}$	32	3.9	12.2	[87]

Fig. 4. Atomic representations of 13 selected MOF structures. Purple ribbons represent surface available for adsorption, calculated using methane as a gas probe. (For interpretation of the references to colour in this figure legend, the reader is referred to the web version of this article.)

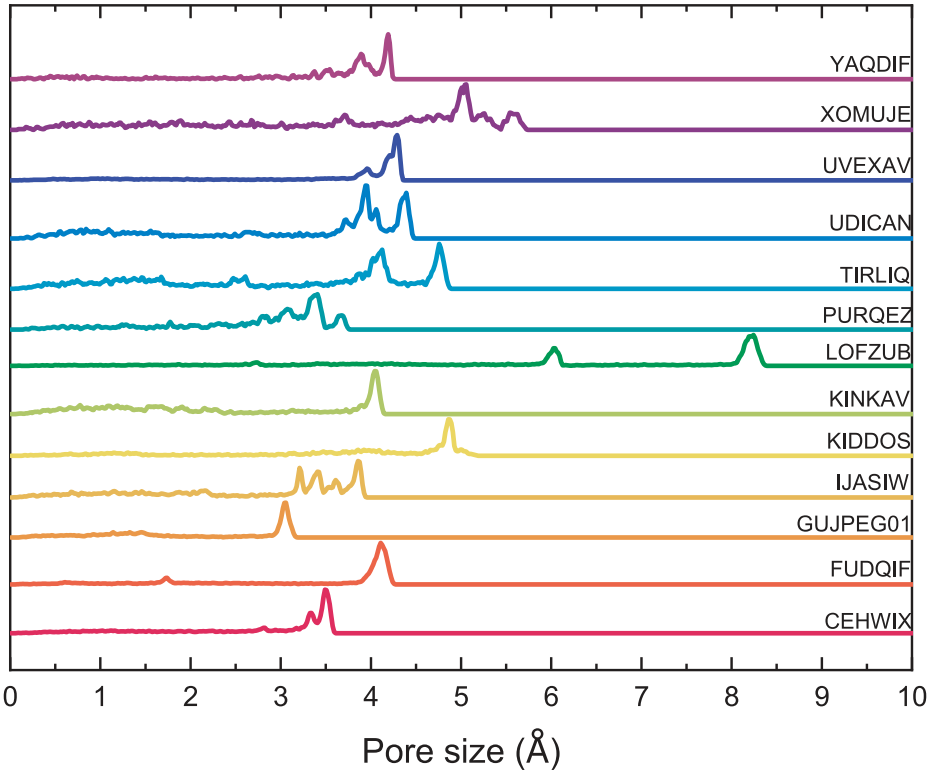

Fig. 5. Pore size distribution for 13 selected MOF structures.

CO_2 and CH_4 indicates the structures more suitable for CO_2/CH_4 mixture separation. In dry conditions the largest differences are observed for FUDQIF (24.9 kJ/mol), GUJPEG01 (20.8 kJ/mol), LOFZUB (21.3 kJ/mol) and UVEXAW (21.0 kJ/mol). CEHWIX, GUJPEG01 and FUDQIF also have the highest selectivity (> 230) in dry conditions (Fig. 6b). The selectivity of UVEXAW is very low in dry conditions (of the order of 6) but increases with humidity of the gas mixture (up to 32.5 for 5% of water content). It should be remembered that to ensure efficient regeneration of the sorbent (desorption of the retained CO_2), the materials should show simultaneously high selectivity and moderate heat of CO_2 adsorption. When the heats of adsorption increases above 17 kJ/mol, the liquefaction of CO_2 inside the pores occurs, making its desorption difficult [90]. Among selected MOFs, all present the heat of CO_2 adsorption above 30 kJ/mol, but for XOMUJE (34.5 kJ/mol), GUJPEG01 (36.5 kJ/mol), IJASIW (36.9 kJ/mol) and PURQEZ (36.9 kJ/mol) the values are the lowest. PURQEZ and GUJPEG01 additionally show the largest difference between CO_2 and CH_4 adsorption heats (16.4 kJ/mol and 20.8 kJ/mol, respectively). The total (CH_4 + CO_2) loading in GUJPEG01 in the absence of water is 1.16 mol/kg, almost 3 times smaller than in PURQEZ (3.71 mol/kg), but the selectivity of GUJPEG01 is an order of magnitude higher. Therefore, GUJPEG01 is the best candidate for an efficient selective sorbent of dry CO_2/CH_4 mixture.

Humidity of the environment is an important aspect to account for when choosing the best sorbent for gas separation in real industrial conditions. Whereas SO_x, NO_x, and particulate matter are usually

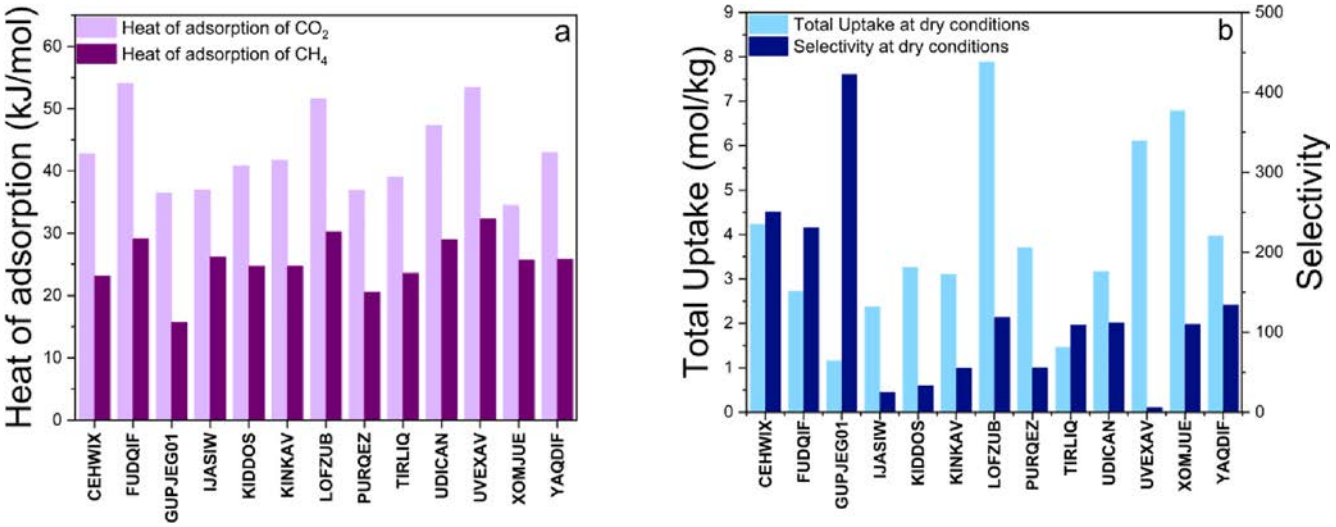

Fig. 6. a) Heat of adsorption for CO_2 (light purple) and CH_4 (dark purple), and b) total uptake (blue) and selectivity (turquoise) of selected structures in dry conditions. (For interpretation of the references to colour in this figure legend, the reader is referred to the web version of this article.)

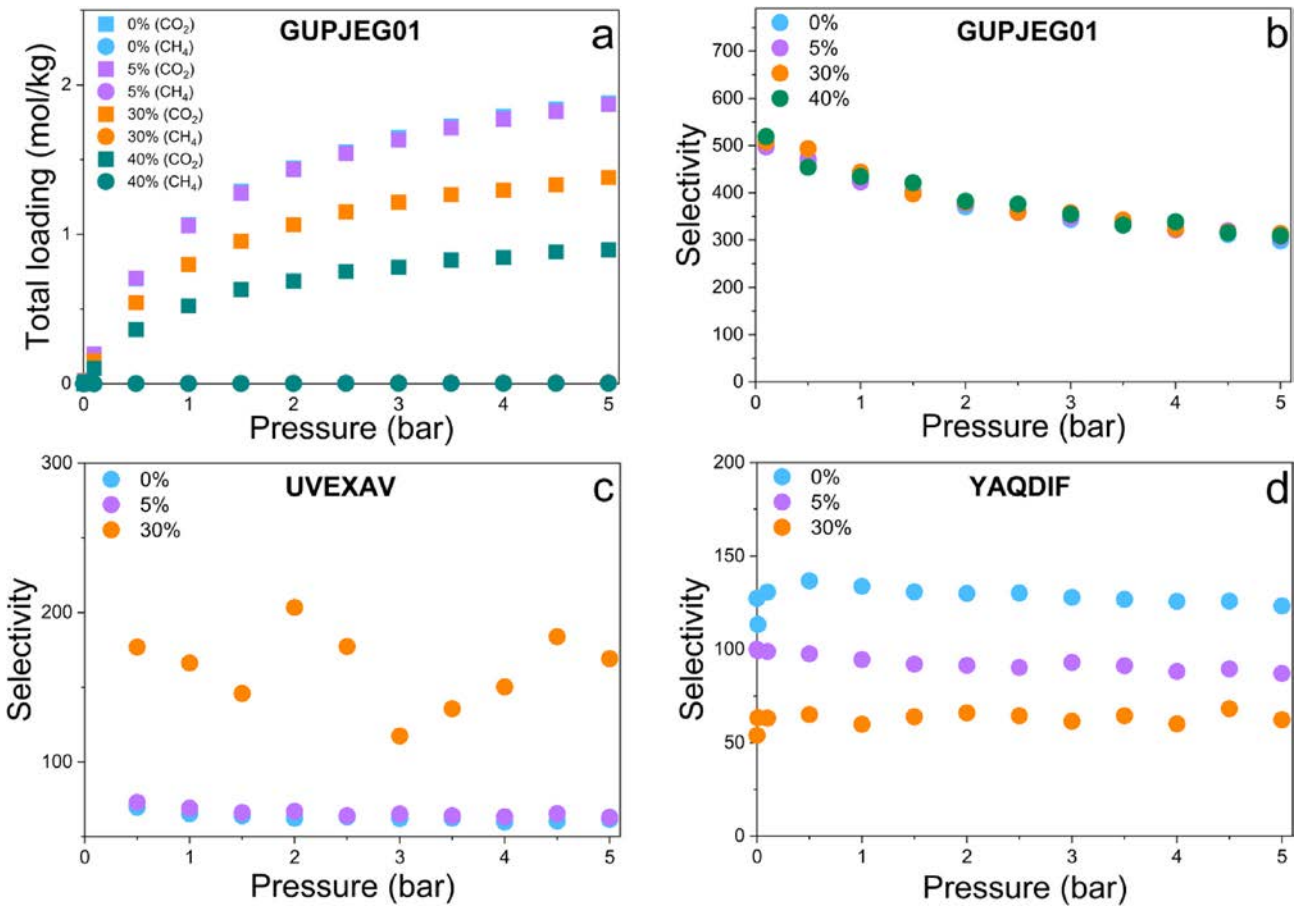

Fig. 7. a) Isotherm of CO_2 and CH_4 adsorption from CO_2/CH_4 mixture in GUJPEG01 for different humidity conditions. b–d:. 3 groups of CO_2/CH_4 selectivity evolution in a function of pressure and humidity: b) no evolution of selectivity with varying humidity (represented by GUJPEG01); c) selectivity increases with increasing humidity (represented by UVEXAV); d) selectivity decreases with increasing humidity (represented by YAQDIF).

effectively removed from biogas by a variety of physical and chemical methods and remaining mixture contains overwhelming majority of CH_4, CO_2, O_2, N_2, and H_2O are still present [91]. Flue gas from the biomethane production may contain between 3% and 20% of water in the total volume of the stream, depending on its source [91,92]. That introduces very specific working conditions for the adsorbent, and highly selective requirement of stability in humid environment.

For all structures, as the humidity of the framework increases, the total adsorbed amount decreases. It is mainly due to the fact that the water inserted into the structure and maintained at the constant level during simulations of CO_2/CH_4 mixture adsorption partially saturates the adsorption sites, and occupies the space geometrically available for adsorption; similar behavior was previously reported in Covalent-Organic Frameworks by Vincent-Luna et. al. [35]. As an example, Fig. 7a shows the isotherms of CO_2 and CH_4 adsorption from CO_2/CH_4 mixture in GUJPEG01. CO_2 adsorbs in the structure at any water content, although its uptake decreases when the humidity increases. On the contrary, CH_4 is almost completely excluded from the structure, at any water content. GUPJEG01 show extremely good separation properties for each of the water contents tested here. The same highly selective adsorption in humid conditions was observed in CEHWIX structure.

The impact of water content on selectivity in the chosen structures is not the same. We identified three groups of behaviors. In the first group of structures the selectivity is independent on structure humidity, but slightly drops at higher gas pressures. Such behavior, observed for GUPJEG01 and UDICAN frameworks (Fig. 7b and Fig. S1 in SI, respectively), is forth seen by industry, as in industrial gas separation processes a constant performance of sorbent in variable humidity conditions is required. It should be noted that the MOFs from this group possess pores of the diameter smaller than (or close to) 3.8 Å, from which accommodation of CH_4 molecules is geometrically excluded. At the same time, however, only small amount of CO_2 can be adsorbed in the structure when the water content in the framework increases.

The second group of materials gather MOF structures in which the selectivity is practically independent on the gas pressure but depends on ambient humidity. Within this category of behaviors two subgroup of structures were distinguished. The first one shows increasing selectivity when the ambient humidity increases. A representative curve of such behavior is shown in Fig. 7c for UVEXAV framework (and in Fig. S2 in SI for PURQEZ). The second category, represented by YAQDIF framework (Fig. 7d), shows lower selectivity in more humid conditions. CEHWIX, another framework from this category, shows one of the highest selectivity and high total uptake in dry conditions (Fig. 6b), and performs well (selectivity > 50) even at 40% of humidity (see Fig. S3 in SI). Therefore, it is one of the most promising candidates for selective CO_2 adsorption from humid CO_2/CH_4 mixture.

FUDQIF structure exhibits the characteristics totally different from other selected MOFs. Its selectivity is strongly pressure dependent: when the gas pressure increases the selectivity decreases (from ~ 350 at 0.5 bar to ~ 100 at 3 bar at dry conditions, see Fig. S4 in SI). This is mainly due to the large amount of CH_4 that the framework can adsorb. As the size of the FUDQIF pores is centered on 4.1 Å (see Fig. 5), the methane adsorption in the structure is not geometrically excluded. At 3 bar CH_4 uptake reaches 0.18 mol/kg, which drastically decreases the value of selectivity. The selectivity is also strongly reduced by humidity: at the gas pressure of 3 bar it becomes negligible when humidity reaches the level of 30%. This suggests that the framework interaction with the dipole moment of water is stronger than its interaction with

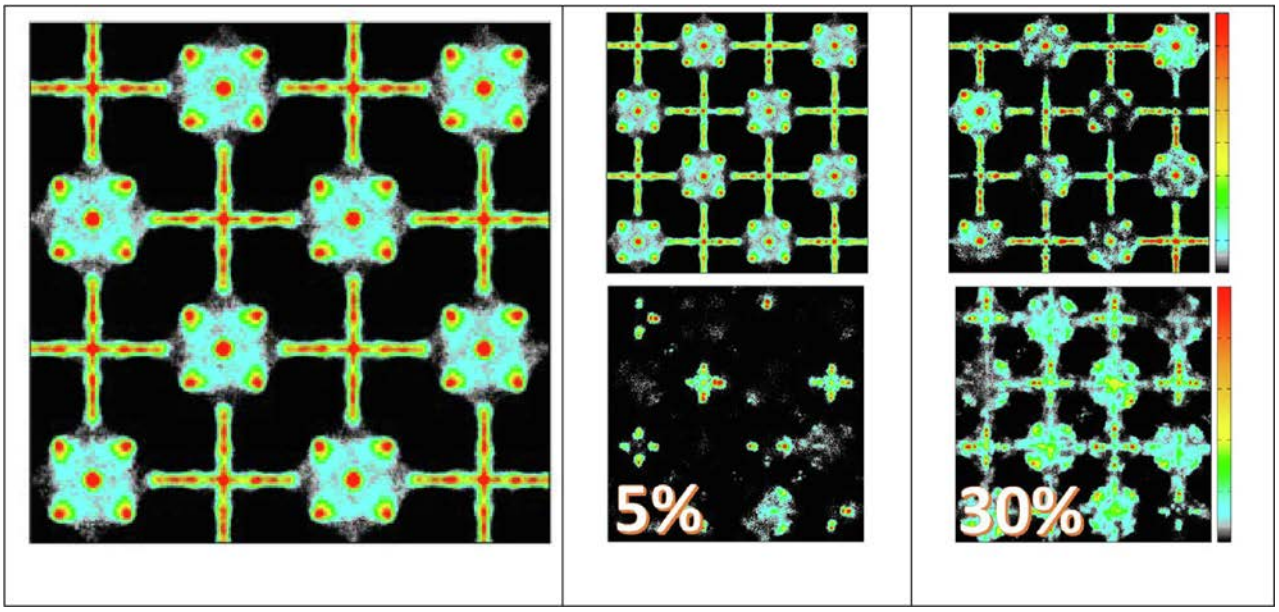

Fig. 8. (left panel):Distribution of CO_2 density in LOFZUB; (middle panel): CO_2(top) and H_2O (bottom) distributions in LOFZUB at 5% of humidity; (right panel): CO_2 (top) and H_2O (bottom)distributions in LOFZUB at 30% of humidity; The colors (from blue to red) denote increasing density of the adsorbed CO_2 (H_2O) molecules. (For interpretation of the references to colour in this figure legend, the reader is referred to the web version of this article.)

CO_2 quadrupole moment. In consequence, water molecules are preferentially adsorbed in the framework, and the volume available for CO_2 adsorption decreases.

Fig. 8 shows the distributions of CO_2 (left panel) and H_2O (right panel) densities in LOFZUB structure for which the selectivity increases with raising humidity (Fig. S5 in SI). This framework (actually, a zeolite) contains 2 types of pores (see Fig. 4), of the largest diameters between the selected structures, centered around 6 Å and 8 Å (see Fig. 5). In the dry structure CO_2 occupies mainly the highly adsorbing sites located in the corners of larger pore, and the center of small pores, where it can fit geometrically. At 5% of humidity the molecules of water introduced to the structure adsorb preferentially in the smaller pores, progressively excluding CO_2 from them. When the humidity increases up to 30% water starts to populate larger pores as well, together with CO_2 molecules. The adsorption selectivity of the system increases, as methane is replaced for water molecules.

4. Conclusions

The results presented in this paper have shown that the numerical screening is powerful methodology which allows one to rapidly select, from a large structures database, systems having the desired separation properties. Starting from nearly 3000 structures, we were able to make a preliminary selection of over 700 potentially suitable MOFs for CO_2/CH_4 separation in the presence of water and then, using GCMC simulations, to refine the choice to 13 structures which perform the best in variable humidity conditions.

The analysis of the selected structures revealed that even in dry conditions the selectivity is not a simple function of the typical porous materials characteristics: accessible volume, enthalpy of adsorption, specific surface area, or pore size distribution. Most probably other structural properties (e.g. specific chemistry of the adsorption sites, particular charge distributions) have to be taken into account. The issue of strong correlations between the separation selectivity and the specific adsorbent properties is an interesting field for more fundamental studies. Therefore, massive numerical screening is the best choice of structure selection method, before the detailed experimental verification of structure's properties starts.

We found that in general structures containing Zn ions in metallic centers and nitrogen atoms in linkers, with ordered, small channels (of the diameter $<$ 8 Å) are more suitable for selective CO_2 adsorption from CO_2/CH_4 mixture at the studied conditions. The best selected materials for the analyzed application are GUPJEG01, CEHWIX (especially in low humidity conditions), and the zeolite LOFZUB. They show high selectivity and total adsorption uptake. In particular, GUPJEG01 show excellent separation properties, almost independent of the water content.

A universal selective sorbent, performing well in dry and wet conditions is difficult to designate. For the selected structures, the selectivity of the framework either increased, decreased, or remained unchanged when the structure humidity was varied between 0% and 40 % of the nominal storage capacity of the structure. The final choice of the most appropriate MOF for the CO_2/CH_4 will depend then on the level of humidity present in starting gas/environment during separation process and in the (p, T) operational conditions.

Declaration of Competing Interest

The authors declare that they have no known competing financial interests or personal relationships that could have appeared to influence the work reported in this paper.

Acknowledgements

B.K., L.F, F.F and J.R. acknowledge support from the Polish National Science Centre (NCN, Grant OPUS No. 2015/17/B/ST8/00099). We thank C3UPO for the HPC support. Calculations have been carried out in Wroclaw Center for Networking and Supercomputing (http://www.wcss.pl), grant no. 33. J.R. would like to thank Bartosz Mazur for in implementing Python scripts for data collection.

Appendix A. Supplementary data

Supplementary data to this article can be found online at https://doi.org/10.1016/j.cej.2020.126392.

References

[1] IEA, https://data.worldbank.org/indicator/eg.use.comm.fo.zs, (n.d.).
[2] D.Y.C. Leung, G. Caramanna, M.M. Maroto-valer, An overview of current status of carbon dioxide capture and storage technologies, Renew. Sustain. Energy Rev. 39 (2014) 426–443, https://doi.org/10.1016/j.rser.2014.07.093.
[3] J.C.M. Pires, F.G. Martins, M.C.M. Alvim-Ferraz, M. Simões, Recent developments on carbon capture and storage: An overview, Chem. Eng. Res. Des. 89 (2011) 1446–1460, https://doi.org/10.1016/j.cherd.2011.01.028.
[4] R.M. Cuéllar-Franca, A. Azapagic, Carbon capture, storage and utilisation technologies: a critical analysis and comparison of their life cycle environmental impacts, J. CO_2 Util. 9 (2015) 82–102, https://doi.org/10.1016/j.jcou.2014.12.001.
[5] H. de Coninck, S.M. Benson, Carbon dioxide capture and storage: issues and prospects, Annu. Rev. Environ. Resour. 39 (2014) 243–270, https://doi.org/10.1146/annurev-environ-032112-095222.
[6] R. Gunderson, D. Stuart, B. Petersen, The fossil fuel industry's framing of carbon capture and storage: faith in innovation, value instrumentalization, and status quo maintenance, J. Clean. Prod. 252 (2020) 119767, , https://doi.org/10.1016/j.jclepro.2019.119767.
[7] D.M. Reiner, Learning through a portfolio of carbon capture and storage demonstration projects, Nat. Energy 1 (2016) 15011–15017, https://doi.org/10.1038/nenergy.2015.11.
[8] S. Sgouridis, M. Carbajales-Dale, D. Csala, M. Chiesa, U. Bardi, Comparative net energy analysis of renewable electricity and carbon capture and storage, Nat. Energy 4 (2019) 456–465, https://doi.org/10.1038/s41560-019-0365-7.
[9] J. Gibbins, H. Chalmers, Carbon capture and storage, Energy Policy 36 (2008) 4317–4322, https://doi.org/10.1016/j.enpol.2008.09.058.
[10] A. Samanta, A. Zhao, G.K.H. Shimizu, P. Sarkar, R. Gupta, Post-combustion CO 2 capture using solid sorbents: a review, Ind. Eng. Chem. Res. 51 (2012) 1438–1463, https://doi.org/10.1021/ie200686q.
[11] Y. Wang, L. Zhao, A. Otto, M. Robinius, D. Stolten, A review of post-combustion CO2 capture technologies from coal-fired power plants, Energy Proc., Elsevier Ltd (2017) 650–665, https://doi.org/10.1016/j.egypro.2017.03.1209.
[12] J.A. Mason, K. Sumida, Z.R. Herm, R. Krishna, J.R. Long, Evaluating metal-organic frameworks for post-combustion carbon dioxide capture via temperature swing adsorption, Energy Environ. Sci. 4 (2011) 3030–3040, https://doi.org/10.1039/c1ee01720a.
[13] R.M. Siqueira, G.R. Freitas, H.R. Peixoto, J.F.D. Nascimento, A.P.S. Musse, A.E.B. Torres, D.C.S. Azevedo, M. Bastos-Neto, Carbon dioxide capture by pressure swing adsorption, Energy Proc. 114 (2017) 2182–2192, https://doi.org/10.1016/j.egypro.2017.03.1355.
[14] R. Ben-Mansour, M.A. Habib, O.E. Bamidele, M. Basha, N.A.A. Qasem, A. Peedikakkal, T. Laoui, M. Ali, Carbon capture by physical adsorption: materials, experimental investigations and numerical modeling and simulations – a review, Appl. Energy 161 (2016) 225–255, https://doi.org/10.1016/j.apenergy.2015.10.011.
[15] K.B. Lee, M.G. Beaver, H.S. Caram, S. Sircar, Reversible chemisorbents for carbon dioxide and their potential applications, Ind. Eng. Chem. Res. 47 (2008) 8048–8062, https://doi.org/10.1021/ie800795y.
[16] P.A. Webley, Adsorption technology for CO2 separation and capture: a perspective, Adsorption 20 (2014) 225–231, https://doi.org/10.1007/s10450-014-9603-2.
[17] Z. Zhang, Y. Zhao, Q. Gong, Z. Li, J. Li, MOFs for CO2 capture and separation from flue gas mixtures: the effect of multifunctional sites on their adsorption capacity and selectivity, Chem. Commun. (Camb.) 49 (2013) 653–661, https://doi.org/10.1039/c2cc35561b.
[18] L.C. Lin, A.H. Berger, R.L. Martin, J. Kim, J.A. Swisher, K. Jariwala, C.H. Rycroft, A.S. Bhown, M.W. Deem, M. Haranczyk, B. Smit, In silico screening of carbon-capture materials, Nat. Mater. 11 (2012) 633–641, https://doi.org/10.1038/nmat3336.
[19] H. Yang, Z. Xu, M. Fan, R. Gupta, R.B. Slimane, A.E. Bland, I. Wright, Progress in carbon dioxide separation and capture: a review, J. Environ. Sci. 20 (2008) 14–27, https://doi.org/10.1016/S1001-0742(08)60002-9.
[20] N. Hedin, L. Andersson, L. Bergström, J. Yan, Adsorbents for the post-combustion capture of CO2 using rapid temperature swing or vacuum swing adsorption, Appl. Energy 104 (2013) 418–433, https://doi.org/10.1016/j.apenergy.2012.11.034.
[21] I. Sárvári Horváth, M. Tabatabaei, K. Karimi, R. Kumar, Recent updates on biogas production – a review, Biofuel Res. J. 3 (2016) 394–402, https://doi.org/10.18331/BRJ2016.3.2.4.
[22] J.F. Vivo-Vilches, A.F. Pérez-Cadenas, F.J. Maldonado-Hódar, F. Carrasco-Marín, R.P.V. Faria, A.M. Ribeiro, A.F.P. Ferreira, A.E. Rodrigues, Biogas upgrading by selective adsorption onto CO2 activated carbon from wood pellets, J. Environ. Chem. Eng. 5 (2017) 1386–1393, https://doi.org/10.1016/j.jece.2017.02.015.
[23] T.C. Drage, O. Kozynchenko, C. Pevida, M.G. Plaza, F. Rubiera, J.J. Pis, C.E. Snape, S. Tennison, Developing activated carbon adsorbents for pre-combustion CO2 capture, Energy Procedia, Elsevier (2009) 599–605, https://doi.org/10.1016/j.egypro.2009.01.079.
[24] K.T. Chue, J.N. Kim, Y.J. Yoo, S.H. Cho, R.T. Yang, Comparison of activated carbon and zeolite 13X for CO2 recovery from flue gas by pressure swing adsorption, Ind. Eng. Chem. Res. 34 (1995) 591–598, https://doi.org/10.1021/ie00041a020.
[25] R. Kumar, C. Zhang, A.K. Itta, W.J. Koros, Highly permeable carbon molecular sieve membranes for efficient CO2/N2 separation at ambient and subambient temperatures, J. Memb. Sci. 583 (2019) 9–15, https://doi.org/10.1016/j.memsci.2019.04.033.
[26] H.H. Tseng, C.T. Wang, G.L. Zhuang, P. Uchytil, J. Reznickova, K. Setnickova, Enhanced H2/CH4 and H2/CO2 separation by carbon molecular sieve membrane coated on titania modified alumina support: effects of TiO2 intermediate layer preparation variables on interfacial adhesion, J. Memb. Sci. 510 (2016) 391–404, https://doi.org/10.1016/j.memsci.2016.02.036.
[27] L.A.M. Rocha, K.A. Andreassen, C.A. Grande, Separation of CO2/CH4 using carbon molecular sieve (CMS) at low and high pressure, Chem. Eng. Sci. 164 (2017) 148–157, https://doi.org/10.1016/j.ces.2017.01.071.
[28] A.E. Amooghin, H. Sanaeepur, M.Z. Pedram, New advances in polymeric membranes for CO2 separation, Polym. Sci. Res. Adv. Pract. Appl. Educ. Asp. (2016) 354–368.
[29] X. Zhu, Y. Hua, C. Tian, C.W. Abney, P. Zhang, T. Jin, G. Liu, K.L. Browning, R.L. Sacci, G.M. Veith, H.-C. Zhou, W. Jin, S. Dai, Accelerating membrane-based CO_2 separation by soluble nanoporous polymer networks produced by mechanochemical oxidative coupling, Angew. Chemie Int. Ed. 57 (2018) 2816–2821, https://doi.org/10.1002/anie.201710420.
[30] Z. Dai, L. Ansaloni, L. Deng, Recent advances in multi-layer composite polymeric membranes for CO2 separation: a review, Green Energy Environ. 1 (2016) 102–128, https://doi.org/10.1016/j.gee.2016.08.001.
[31] M.L. Carreon, S. Li, M.A. Carreon, AlPO-18 membranes for CO2/CH4 separation, Chem. Commun. 48 (2012) 2310–2312, https://doi.org/10.1039/c2cc17249f.
[32] Q. Liu, N.C.O. Cheung, A.E. Garcia-Bennett, N. Hedin, Aluminophosphates for CO2 separation, ChemSusChem 4 (2011) 91–97, https://doi.org/10.1002/cssc.201000256.
[33] I. Deroche, L. Gaberova, G. Maurin, P. Llewellyn, M. Castro, P. Wright, Adsorption of carbon dioxide in SAPO STA-7 and AlPO-18: Grand Canonical Monte Carlo simulations and microcalorimetry measurements, Adsorption. 14 (2008) 207–213, https://doi.org/10.1007/s10450-007-9098-1.
[34] H. Li, M. Eddaoudi, M. O'Keeffe, O.M. Yaghi, Design and synthesis of an exceptionally stable and highly porous metal-organic framework, Nature 402 (1999) 276–279, https://doi.org/10.1038/46248.
[35] J.M. Vicent-Luna, A. Luna-Triguero, S. Calero, Storage and separation of carbon dioxide and methane in hydrated covalent organic frameworks, J. Phys. Chem. C 120 (2016) 23756–23762, https://doi.org/10.1021/acs.jpcc.6b05233.
[36] S.K. Henninger, H.A. Habib, C. Janiak, MOFs as adsorbents for low temperature heating and cooling applications, J. Am. Chem. Soc. 131 (2009) 2776–2777, https://doi.org/10.1021/ja808444z.
[37] W. Xuan, C. Zhu, Y. Liu, Y. Cui, Mesoporous metal-organic framework materials, Chem. Soc. Rev. 41 (2012) 1677–1695, https://doi.org/10.1039/c1cs15196g.
[38] J. Lee, O.K. Farha, J. Roberts, K.A. Scheidt, S.T. Nguyen, J.T. Hupp, Metal–organic framework materials as catalysts, Chem. Soc. Rev. 38 (2009) 1450, https://doi.org/10.1039/b807080f.
[39] S.R. Batten, N.R. Champness, X.-M. Chen, J. Garcia-Martinez, S. Kitagawa, L. Öhrström, M. O'Keeffe, M. Paik Suh, J. Reedijk, Terminology of metal–organic frameworks and coordination polymers (IUPAC Recommendations 2013), Pure Appl. Chem. 85 (2013) (2013) 1715–1724, https://doi.org/10.1351/PAC-REC-12-11-20.
[40] Z.-Y. Gu, C.-X. Yang, N. Chang, X.-P. Yan, Metal-organic frameworks for analytical chemistry: from sample collection to chromatographic separation, Acc. Chem. Res. 734 (2012) 734–745, https://doi.org/10.1021/ar2002599.
[41] C. Janiak, J.K. Vieth, MOFs, MILs and more: concepts, properties and applications for porous coordination networks (PCNs), New J. Chem. 34 (2010) 2366, https://doi.org/10.1039/c0nj00275e.
[42] I. Senkovska, S. Kaskel, Ultrahigh porosity in mesoporous MOFs: promises and limitations, Chem. Commun. 50 (2014) 7089, https://doi.org/10.1039/c4cc00524d.
[43] M. Alhamami, H. Doan, C.H. Cheng, A review on breathing behaviors of metal-organic-frameworks (MOFs) for gas adsorption, Materials (Basel). 7 (2014) 3198–3250, https://doi.org/10.3390/ma7043198.
[44] J. Gascon, A. Corma, F. Kapteijn, F.X. Llabrés, I. Xamena, Metal organic framework catalysis: quo vadis? ACS Catal. 4 (2014) 361–378, https://doi.org/10.1021/cs400959k.
[45] S.S. Han, S.H. Choi, A.C.T. Van Duin, Molecular dynamics simulations of stability of metal-organic frameworks against H2O using the ReaxFF reactive force field, Chem. Commun. 46 (2010) 5713–5715, https://doi.org/10.1039/c0cc01132k.
[46] Y. Cui, Y. Yue, G. Qian, B. Chen, Luminescent functional metal-organic frameworks, Chem. Rev. 112 (2012) 1126–1162, https://doi.org/10.1021/cr200101d.
[47] J.A. Coelho, A.M. Ribeiro, A.F.P. Ferreira, S.M.P. Lucena, A.E. Rodrigues, D.C.S. De Azevedo, Stability of an Al-Fumarate MOF and its potential for CO2 capture from wet stream, Ind. Eng. Chem. Res. 55 (2016) 2134–2143, https://doi.org/10.1021/acs.iecr.5b03509.
[48] Z.-Y. Gu, J.-Q. Jiang, X.-P. Yan, Fabrication of isoreticular metalàorganic framework coated capillary columns for high-resolution gas chromatographic separation of persistent organic pollutants, Anal Chem. 83 (2011) 5093–5100, https://doi.org/10.1021/ac200646w.
[49] H. Demir, C.J. Cramer, J.I. Siepmann, Computational screening of metal-organic frameworks for biogas purification, Mol. Syst. Des. Eng. 4 (2019) 1125–1135, https://doi.org/10.1039/c9me00095j.
[50] S. Cavenati, C.A. Grande, A.E. Rodrigues, C. Kiener, U. Müller, Metal organic framework adsorbent for biogas upgrading, Ind. Eng. Chem. Res. 47 (2008) 6333–6335, https://doi.org/10.1021/ie8005269.
[51] S. Li, Y.G. Chung, R.Q. Snurr, High-throughput screening of metal-organic frameworks for CO_2 capture in the presence of water, Langmuir 32 (2016) 10368–10376, https://doi.org/10.1021/acs.langmuir.6b02803.
[52] H. Huang, W. Zhang, D. Liu, C. Zhong, Understanding the effect of trace amount of water on CO_2 capture in natural gas upgrading in metal-organic frameworks: a molecular simulation study, Ind. Eng. Chem. Res. 51 (2012) 10031–10038, https://doi.org/10.1021/ie202699r.

[53] J. Yu, P.B. Balbuena, Water effects on postcombustion Co2 capture in Mg-MOF-74, J. Phys. Chem. C 117 (2013) 3383–3388, https://doi.org/10.1021/jp311118x.

[54] S. Han, Y. Huang, T. Watanabe, S. Nair, K.S. Walton, D.S. Sholl, J. Carson Meredith, MOF stability and gas adsorption as a function of exposure to water, humid air, SO2, and NO2, Microporous Mesoporous Mater. 173 (2013) 86–91, https://doi.org/10.1016/j.micromeso.2013.02.002.

[55] P. Canepa, C.A. Arter, E.M. Conwill, D.H. Johnson, B.A. Shoemaker, K.Z. Soliman, T. Thonhauser, High-throughput screening of small-molecule adsorption in MOF, J. Mater. Chem. A 1 (2013) 13597–13604, https://doi.org/10.1039/c3ta12395b.

[56] C. Altintas, S. Keskin, Role of partial charge assignment methods in high-throughput screening of MOF adsorbents and membranes for CO2/CH4 separation, Mol. Syst. Des. Eng. 5 (2020) 532–543, https://doi.org/10.1039/c9me00163h.

[57] J. Canivet, A. Fateeva, Y. Guo, B. Coasne, D. Farrusseng, Water adsorption in MOFs: Fundamentals and applications, Chem. Soc. Rev. 43 (2014) 5594–5617, https://doi.org/10.1039/c4cs00078a.

[58] I. Erucar, S. Keskin, Unlocking the effect of H2O on CO2 separation performance of promising MOFs using atomically detailed simulations, Ind. Eng. Chem. Res. 59 (2020) 3141–3152, https://doi.org/10.1021/acs.iecr.9b05487.

[59] S. Keskin, Screening for selectivity, Nat. Energy 5 (2020) 8–9, https://doi.org/10.1038/s41560-019-0514-z.

[60] G. Avci, S. Velioglu, S. Keskin, High-throughput screening of MOF adsorbents and membranes for H2 purification and CO2 capture, ACS Appl. Mater. Interfaces 10 (2018) 33693–33706, https://doi.org/10.1021/acsami.8b12746.

[61] A.N.V. Azar, S. Velioglu, S. Keskin, Large-scale computational screening of metal organic framework (MOF) membranes and MOF-based polymer membranes for H2/N2 separations, ACS Sustain. Chem. Eng. 7 (2019) 9525–9536, https://doi.org/10.1021/acssuschemeng.9b01020.

[62] H. Daglar, S. Keskin, High-throughput screening of metal organic frameworks as fillers in mixed matrix membranes for flue gas separation, Adv. Theory Simulations. 2 (2019) 1900109, https://doi.org/10.1002/adts.201900109.

[63] C. Altintas, S. Keskin, Molecular simulations of MOF membranes and performance predictions of MOF/polymer mixed matrix membranes for CO_2/CH_4 separations, ACS Sustain. Chem. Eng. 7 (2019) 2739–2750, https://doi.org/10.1021/acssuschemeng.8b05832.

[64] A. Ahmed, S. Seth, J. Purewal, A.G. Wong-Foy, M. Veenstra, A.J. Matzger, D.J. Siegel, Exceptional hydrogen storage achieved by screening nearly half a million metal-organic frameworks, Nat. Commun. 10 (2019) 1–9, https://doi.org/10.1038/s41467-019-09365-w.

[65] A.D. Evans, M.S. Cummings, R. Luebke, M.S. Brown, S. Favero, M.P. Attfield, F. Siperstein, D. Fairen-Jimenez, K. Hellgardt, R. Purves, D. Law, C. Petit, Screening metal-organic frameworks for dynamic CO/N2 separation using complementary adsorption measurement techniques, Ind. Eng. Chem. Res. 58 (2019) 18336–18344, https://doi.org/10.1021/acs.iecr.9b03724.

[66] S. Han, Y. Huang, T. Watanabe, Y. Dai, K.S. Walton, S. Nair, D.S. Sholl, J.C. Meredith, High-throughput screening of metal-organic frameworks for CO_2 separation, ACS Comb. Sci. 14 (2012) 263–267, https://doi.org/10.1021/co3000192.

[67] N. Chanut, S. Bourrelly, B. Kuchta, C. Serre, J.S. Chang, P.A. Wright, P.L. Llewellyn, Screening the effect of water vapour on gas adsorption performance: application to CO2 capture from flue gas in metal-organic frameworks, ChemSusChem 10 (2017) 1543–1553, https://doi.org/10.1002/cssc.201601816.

[68] D. Nazarian, J.S. Camp, D.S. Sholl, A comprehensive set of high-quality point charges for simulations of metal-organic frameworks, Chem. Mater. 28 (2016) 785–793, https://doi.org/10.1021/acs.chemmater.5b03836.

[69] I. Matito-Martos, P.Z. Moghadam, A. Li, V. Colombo, J.A.R. Navarro, S. Calero, D. Fairen-Jimenez, Discovery of an optimal porous crystalline material for the capture of chemical warfare agents, Chem. Mater. 30 (2018) 4571–4579, https://doi.org/10.1021/acs.chemmater.8b00843.

[70] C.R. Groom, I.J. Bruno, M.P. Lightfoot, S.C. Ward, The cambridge structural database, Acta Crystallogr Sect. B Struct. Sci. Cryst. Eng. Mater. 72 (2016) 171–179, https://doi.org/10.1107/S2052520616003954.

[71] A.K. Rappe, C.J. Casewit, K.S. Colwell, W.A. Goddard, W.M. Skiff, UFF, a full periodic table force field for molecular mechanics and molecular dynamics simulations, J. Am. Chem. Soc. 114 (1992) 10024–10035, https://doi.org/10.1021/ja00051a040.

[72] S.L. Mayo, B.D. Olafson, W.A. Goddard, DREIDING: a generic force field for molecular simulations, J. Phys. Chem. 94 (1990) 8897–8909, https://doi.org/10.1021/j100389a010.

[73] A. García-Sánchez, C.O. Ania, J.B. Parra, D. Dubbeldam, T.J.H. Vlugt, R. Krishna, S. Calero, Transferable force field for carbon dioxide adsorption in zeolites, J. Phys. Chem. C 113 (2009) 8814–8820, https://doi.org/10.1021/jp810871f.

[74] W.L. Jorgensen, J. Chandrasekhar, J.D. Madura, R.W. Impey, M.L. Klein, Comparison of simple potential functions for simulating liquid water, J. Chem. Phys. 79 (1983) 926–935, https://doi.org/10.1063/1.445869.

[75] Q. Yang, J.P. Zhao, Z.Y. Liu, Single crystal to single crystal transition in (10, 3)-d framework with pyrazine-2-carboxylate ligand: synthesis, structures and magnetism, J. Solid State Chem. 196 (2012) 52–57, https://doi.org/10.1016/j.jssc.2012.07.050.

[76] M. Feyand, M. Köppen, G. Friedrichs, N. Stock, Bismuth tri- and tetraarylcarboxylates: crystal structures, in situ X-ray diffraction, intermediates and luminescence, Chem. – A Eur. J. 19 (2013) 12537–12546, https://doi.org/10.1002/chem.201301139.

[77] R. Singh, P.K. Bharadwaj, Coordination polymers built with a linear bis-imidazole and different dicarboxylates: unusual entanglement and emission properties, Cryst. Growth Des. 13 (2013) 3722–3733, https://doi.org/10.1021/cg400756z.

[78] S.A. Sapchenko, D.G. Samsonenko, V.P. Fedin, Synthesis, structure and luminescent properties of metal-organic frameworks constructed from unique Zn- and Cd-containing secondary building blocks, Polyhedron 55 (2013) 179–183, https://doi.org/10.1016/j.poly.2013.03.031.

[79] Y. Si, H. Chen, C. Chen, [1,2-Bis(diphenylphosphanyl)ethane-2κ2P, P′] tetracarbonyl-1κ3C,2κC-(μ-2-cyclopentyl-2-azapropane- 1,3-dithiolato-1:24 S, S′:S, S′) diiron(II)(Fe-Fe), Acta Crystallogr Sect. E Struct. Reports Online 67 (2011) m1500–m1501, https://doi.org/10.1107/S1600536811040347.

[80] R. Hajjar, C. Volkringer, T. Loiseau, N. Guillou, J. Marrot, G. Férey, I. Margiolaki, G. Fink, C. Morais, F. Taulelle, 71Ga Slow-CTMAS NMR and crystal structures of MOF-type gallium carboxylates with infinite edge-sharing octahedra chains (MIL-120 and MIL-124), Chem. Mater. 23 (2011) 39–47, https://doi.org/10.1021/cm1025427.

[81] K. Uemura, A. Maeda, T.K. Maji, P. Kanoo, H. Kita, Syntheses, crystal structures and adsorption properties of ultramicroporous coordination polymers constructed from hexafluorosilicate ions and pyrazine, Eur. J. Inorg. Chem. 2009 (2009) 2329–2337, https://doi.org/10.1002/ejic.200900144.

[82] P.A. Wright, M.J. Maple, A.M.Z. Slawin, V. Patinec, R. Alan Aitken, S. Welsh, P.A. Cox, Cation-directed syntheses of novel zeolite-like metalloaluminophosphates STA-6 and STA-7 in the presence of azamacrocycle templates, J. Chem. Soc. Dalt. Trans. (2000) 1243–1248, https://doi.org/10.1039/a909249h.

[83] B.S. Luisi, Z. Ma, B. Moulton, Tri-metal secondary building units: toward the design of thermally robust crystalline coordination polymers, J. Chem. Crystallogr. 37 (2007) 743–747, https://doi.org/10.1007/s10870-007-9244-3.

[84] Y. Cui, H.L. Ngo, P.S. White, W. Lin, Homochiral 3D lanthanide coordination networks with an unprecedented 4966 topology, Chem. Commun. 2 (2002) 1666–1667, https://doi.org/10.1039/b204249e.

[85] H. Zeng, T. Li, Z. Yan, S. Luo, F. Li, Two porous metal-organic frameworks showing different behaviors to sodium cation, Cryst. Growth Des. 10 (2010) 475–478, https://doi.org/10.1021/cg901114e.

[86] H. He, D. Yuan, H. Ma, D. Sun, G. Zhang, H.C. Zhou, Control over interpenetration in lanthanide-organic frameworks: synthetic strategy and gas-adsorption properties, Inorg. Chem. 49 (2010) 7605–7607, https://doi.org/10.1021/ic100822s.

[87] E. Tynan, P. Jensen, P.E. Kruger, A.C. Lees, Solvent templated synthesis of metal–organic frameworks: structural characterisation and properties of the 3D network isomers ([Mn(dcbp)]·½DMF)n and ([Mn(dcbp)]·2H2O)n, Chem. Commun. 4 (2004) 776–777, https://doi.org/10.1039/b315483a.

[88] D. Dubbeldam, S. Calero, T.J.H. Vlugt, iRASPA: GPU-accelerated visualization software for materials scientists, Mol. Simul. 44 (2018) 653–676, https://doi.org/10.1080/08927022.2018.1426855.

[89] T.J.H. Vlugt, E. García-Pérez, D. Dubbeldam, S. Ban, S. Calero, Computing the heat of adsorption using molecular simulations: the effect of strong Coulombic interactions, J. Chem. Theory Comput. 4 (2008) 1107–1118, https://doi.org/10.1021/ct700342k.

[90] S. Keskin, T.M. van Heest, D.S. Sholl, Can metal-organic framework materials play a useful role in large-scale carbon dioxide separations? ChemSusChem 3 (2010) 879–891, https://doi.org/10.1002/cssc.201000114.

[91] I. Angelidaki, L. Treu, P. Tsapekos, G. Luo, S. Campanaro, H. Wenzel, P.G. Kougias, Biogas upgrading and utilization: current status and perspectives, Biotechnol. Adv. 36 (2018) 452–466, https://doi.org/10.1016/j.biotechadv.2018.01.011.

[92] I. Ullah Khan, M. Hafiz Dzarfan Othman, H. Hashim, T. Matsuura, A.F. Ismail, M. Rezaei-DashtArzhandi, I. Wan Azelee, Biogas as a renewable energy fuel – a review of biogas upgrading, utilisation and storage, Energy Convers. Manag. 150 (2017) 277–294, https://doi.org/10.1016/j.enconman.2017.08.035.